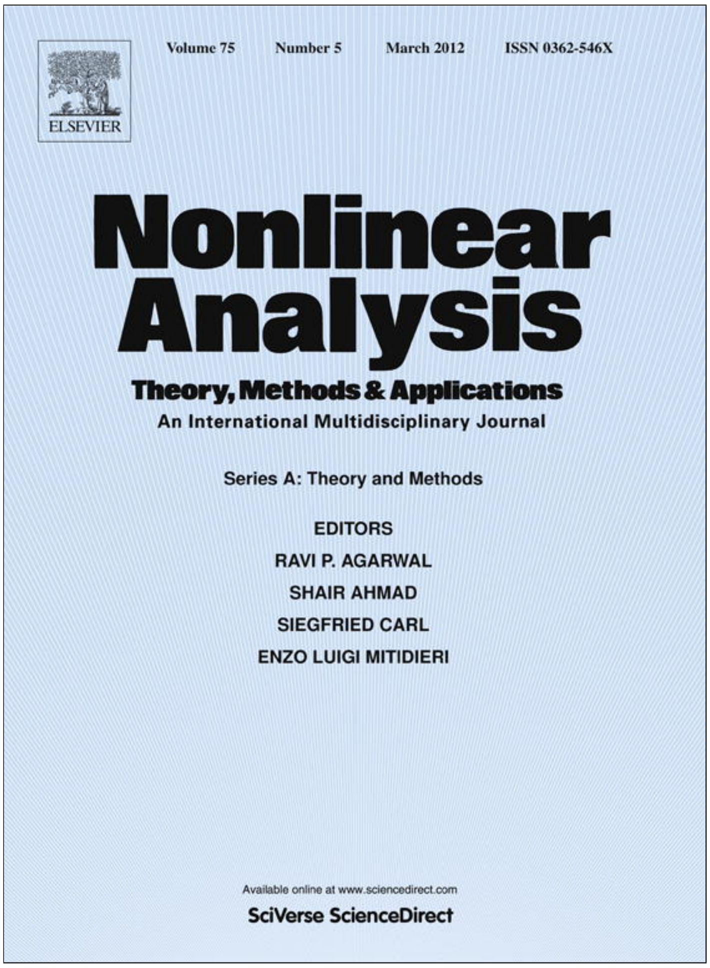
Volume 75 Number 5 March 2012 ISSN 0362-546X

ELSEVIER

Nonlinear Analysis

Theory, Methods & Applications

An International Multidisciplinary Journal

Series A: Theory and Methods

Nonlinear Analysis 75 (2012) 2883–2896

Contents lists available at SciVerse ScienceDirect

Nonlinear Analysis

journal homepage: www.elsevier.com/locate/na

Decay of solutions to a viscous asymptotical model for waterwaves: Kakutani–Matsuuchi model

Min Chen [a,*], Serge Dumont [b], Olivier Goubet [b]

[a] Purdue University, West Lafayette, IN 47907, USA

[b] LAMFA CNRS UMR 6140, Université de Picardie Jules Verne, 33, rue Saint-Leu, 80 039 Amiens, France

ARTICLE INFO

Article history:
Received 19 October 2010
Accepted 27 November 2011
Communicated by Ravi Agarwal

MSC:
35Q35
35Q53
76B15
65M70

Keywords:
Water waves
Viscous asymptotical models
Long-time asymptotics
Non-local operator

ABSTRACT

In this article, we study a viscous asymptotical model equation for water waves

$$u_t + u_x - \beta u_{txx} + \nu\left(D^{\frac{1}{2}}u + \mathcal{F}^{-1}(i\mid\xi\mid^{\frac{1}{2}}\,\mathrm{sgn}(\xi)\widehat{u}(\xi))\right) + \gamma u u_x = 0$$

proposed in Kakutani and Matsuuchi (1975) [6]. Theoretical questions including the existence and regularity of the solutions will be answered. Numerical simulations of its solutions will be carried out and the effects of various parameters will be investigated. We will also predict the decay rate of its solutions towards the equilibrium.

1. Introduction

Modeling the effect of viscosity on gravity waves is a challenging issue. Researches on the subject have been going on for centuries, but have intensified during last decade. For example, [1,2] have derived, independently, asymptotical models for long gravity waves on viscous shallow water. Numerical and theoretical investigations on related equations have been carried out in [3–5]. In this article we will go back in history and study the model equation that appeared in the seminal article of Kakutani and Matsuuchi [6], but in its regularized (or BBM) form

$$u_t + u_x - \beta u_{txx} + \nu\left(D^{\frac{1}{2}}u + \mathcal{F}^{-1}(i|\xi|^{\frac{1}{2}}\,\mathrm{sgn}(\xi)\widehat{u}(\xi))\right) + \gamma u u_x = 0. \tag{1}$$

The effect of the viscous layer is modeled by a nonlocal term that acts as dissipation *and* dispersion, as revealed by the linear dispersion analysis [6]. From the linear dispersion analysis (see also [5]), this model is equivalent to those quoted above at leading orders. These models are generalizations of the well-known Korteweg–de Vries (KdV) and Benjamin–Bona–Mahony (BBM) equations, in which the viscosity is not considered.

* Corresponding author.
E-mail addresses: chen@math.purdue.edu (M. Chen), serge.dumont@u-picardie.fr (S. Dumont), olivier.goubet@u-picardie.fr (O. Goubet).

0362-546X/$ – see front matter © 2011 Elsevier Ltd. All rights reserved.
doi:10.1016/j.na.2011.11.030

The purpose of the article is to study the Kakutani–Matsuuchi equation and to compute numerically the decay rate of its solutions towards equilibrium. In Eq. (1), ν is the viscosity parameter (as in the original Navier–Stokes equations, up to some normalization), β and γ are parameters devoted to balance or unbalance the effects of the geometric dispersion and the nonlinearity. Here and in the sequel $D = (-\Delta)^{\frac{1}{2}}$ is the fractional dissipation operator, and the sign function is defined in the usual way as $\mathrm{sgn}(\xi) = 1$ if $\xi > 0$, $\mathrm{sgn}(0) = 0$, and $\mathrm{sgn}(\xi) = -1$ if $\xi < 0$.

Three different models have been derived in [6] according to a competition between geometrical dispersion (the term βu_{txx}) and dispersion provided by the viscous boundary layer (the nonlocal term). Denoting k as the wave number of the long wave, the different regimes read as follows [6]

- if $\nu \ll k^5$, we are back to KdV type equations and the viscosity effects can be neglected;
- if $\nu \sim k^5$, there is a balance between the geometrical and the viscous dispersion and the equation reads

$$u_t + u_x + \beta u_{xxx} + \nu\left(D^{\frac{1}{2}} u + \mathcal{F}^{-1}(i|\xi|^{\frac{1}{2}}\mathrm{sgn}(\xi)\widehat{u}(\xi))\right) + \gamma u u_x = 0, \tag{2}$$

  or, equivalently, in the BBM form (1);
- if $\nu \gg k^5$, only the viscosity really matters and we have

$$u_t + u_x + \nu D^{\frac{1}{2}} u + \nu \mathcal{F}^{-1}\left(i|\xi|^{\frac{1}{2}}\mathrm{sgn}(\xi)\widehat{u}(\xi)\right) + \gamma u u_x = 0. \tag{3}$$

The issue of analyzing the decay rate for solutions to dispersive-dissipative equations was first addressed in the pioneering work [3] for the KdV–Burgers equation. The Kakutani–Matsuuchi equation differs since both dissipation and dispersion are modeled by non-local pseudo-differential operators. The decay rate for a general class of dispersive-dissipative equations with nonlocal operators was addressed in [4,7]; the method is very interesting and takes part of renormalization group methods. Unfortunately, the Kakutani–Matsuuchi equation does not belong to that class whose dissipations read D^b for $b > 1$.

This article is organized as follows. In Section 2, we address some theoretical issues about the initial value problem for Eqs. (2) and (3), and we prove an energy equality that shows that the solution decays to 0 when t goes to $+\infty$. Unfortunately we are not able to prove that the solutions of the full equation decay at the same rate as the solutions to the linearized equation, which is expected in this case. But it is interesting to note that if we consider a formally equivalent equation which has a similar non-local term which is in time instead of in space, then we are able to prove the decay rate for the non-linear equation (see [5] for detail). Hence we handle this issue numerically. In Section 3, we discuss carefully the issues related to the space approximation of the PDE by spectral methods using Fourier expansions. In the last section, we analyze numerically the decay rate of the solutions.

Let us introduce some notations. $H^1(\mathbb{R})$ or for short H^1_x denotes the usual Sobolev space. $\dot{H}^\alpha(\mathbb{R})$ or $\dot{H}^\alpha_x$ is the space of tempered distributions u such that $D^\alpha u$ belongs to $L^2(\mathbb{R})$. The Fourier transform of a function reads

$$\widehat{u}(\xi) = \mathcal{F}(u)(\xi) = \int_{\mathbb{R}} u(x)\exp(-ix\xi)dx.$$

2. Some theoretical results about the Kakutani–Maatsuchi equation

Right now we shall consider the initial value problem of the Kakutani–Matsuuchi equation in its regularized long-wave form (1) as

$$u_t + u_x - \beta u_{txx} + \nu_1 D^{\frac{1}{2}} u + \nu_2 \mathcal{F}^{-1}\left(i|\xi|^{\frac{1}{2}}\mathrm{sgn}(\xi)\widehat{u}(\xi)\right) + \gamma u u_x = 0, \tag{4}$$

where β is a small parameter. This class of equation contains the KM equation for $\nu_1 = \nu_2$ and the Ott–Sudan equation for $\nu_2 = 0$ [8]. We also write our equation in a synthetical way as follows

$$u_t + u_x - \beta u_{txx} + \nu_1 D^{\frac{1}{2}} u + \nu_2 D^{-\frac{1}{2}} u_x + \gamma u u_x = 0. \tag{5}$$

For the sake of simplicity in notation, we will take $\nu_1 = \nu_2 = \gamma = 1$ unless they are specified.

2.1. $\beta > 0$

For the equations with $\beta > 0$, we will establish the following existence, uniqueness and regularity result.

Proposition 2.1. *For any initial data u_0 in $H^1(\mathbb{R})$, the Eq. (4) with $\beta > 0$ has a unique solution in $C(0, +\infty; H^1(\mathbb{R})) \cap L^2(0, +\infty; \dot{H}^{\frac{1}{4}}(\mathbb{R}))$.*

Proof. To begin, we first consider the linear equation

$$u_t - \beta u_{txx} + \Lambda u = 0, \tag{6}$$

where $\Lambda u = D^{\frac{1}{2}}u + D^{-\frac{1}{2}}u_x + u_x$. Let $A = (1-\beta\Delta)^{-1}\Lambda$ whose symbol is $\frac{(1+i\text{sgn}(\xi))|\xi|^{\frac{1}{2}}+i\xi}{1+\beta\xi^2}$, (6) reads $u_t + Au = 0$ and can be solved in Fourier space with $\widehat{u}(t,\xi) = \exp\left(-t\frac{(1+i\text{sgn}(\xi))|\xi|^{\frac{1}{2}}+i\xi}{1+\beta\xi^2}\right)\widehat{u}_0(\xi)$. Since

$$\left|\exp\left(-t\frac{(1+i\text{sgn}(\xi))|\xi|^{\frac{1}{2}}+i\xi}{1+\beta\xi^2}\right)\right| \le 1,$$

the linear evolution semi-group e^{-tA} is continuous on any Sobolev space $H^k(\mathbb{R})$. Now, for the nonlinear Eq. (4) which reads

$$u_t + Au = (1-\beta\Delta)^{-1}\partial_x\left(\frac{u^2}{2}\right),$$

we seek a *mild* solution. This amounts to solve a fixed point problem in the Duhamel's form

$$u(t) = \exp(-tA)u_0 - \int_0^t \exp((s-t)A)(1-\beta\Delta)^{-1}\partial_x\left(\frac{u^2}{2}\right)ds. \tag{7}$$

This task is easy since $(1-\beta\Delta)^{-1}\partial_x$ is a smoothing operator that maps $H^1(\mathbb{R})$ into $H^1(\mathbb{R})$ (and even $H^2(\mathbb{R})$). Set $R = 2\|u_0\|_{H^1(\mathbb{R})}$, we shall prove that for t small enough the map

$$\mathcal{T}(u) = \exp(-tA)u_0 - \int_0^t \exp((s-t)A)(1-\beta\Delta)^{-1}\partial_x\left(\frac{u^2}{2}\right)ds, \tag{8}$$

maps $B_{H^1_x}(0,R)$, the closed ball centered at 0 with radius R, into itself and is a strict contraction in the complete metric space $C(0,t;B_{H^1_x}(0,R))$. Since $\frac{|\xi|}{1+\beta\xi^2} \le \frac{1}{2\sqrt{\beta}}$,

$$\left\|\exp((s-t)A)(1-\beta\Delta)^{-1}\partial_x\left(\frac{u^2}{2}\right)\right\|_{H^1_x} \le \frac{1}{4\sqrt{\beta}}\|u^2\|_{H^1_x} \le \frac{1}{2\sqrt{\beta}}\|u\|^2_{H^1_x}, \tag{9}$$

yields

$$\|\mathcal{T}(u)\|_{H^1_x} \le \|u_0\|_{H^1_x} + \left|\int_0^T \frac{1}{2\sqrt{\beta}}\|u(s)\|^2_{H^1_x}ds\right| \le \frac{R}{2} + \frac{R^2T}{2\sqrt{\beta}}. \tag{10}$$

Therefore for $RT \le \sqrt{\beta}$, $\mathcal{T}$ maps the ball $B_{H^1_x}(0,R)$ into itself, and the Banach space $C(0,t;B_{H^1_x}(0,R))$ into itself as well. The proof for $\mathcal{T}$ being a strict contraction is similar and is omitted. Hence we have a local *mild* solution. This *mild* solution is also a weak solution in the distribution sense since the map $t \mapsto (1-\beta\Delta)^{-1}\partial_x\left(\frac{u^2}{2}\right)$ is continuous with values in $H^1(\mathbb{R})$.

To prove that this local solution extends to a global solution we prove some a priori estimates on the solution. The idea is to regularize the initial datum, approximating u_0 with functions in the Schwartz class, to compute some energy equalities on these family of approximate solutions and to pass to the limit to prove the energy estimate for u_0 in H^1_x; once again, the process is standard and omitted for the sake of conciseness. We just indicate how to derive formally the energy estimates.

Multiply the Eq. (5) by u and integrate over $\mathbb{R}$ to obtain, since $\int_{\mathbb{R}}(u_x + D^{-\frac{1}{2}}u_x + uu_x)udx = 0$ and

$$\frac{1}{2}\frac{d}{dt}(\|u\|^2_{L^2_x} + \beta\|u_x\|^2_{L^2_x}) + \|D^{\frac{1}{4}}u\|^2_{L^2_x} = 0, \tag{11}$$

that

$$\|u(t)\|^2_{L^2} + \beta\|u_x(t)\|^2_{L^2} + 2\int_0^t \|D^{\frac{1}{4}}u(s)\|^2_{L^2_x}ds = \|u_0\|^2_{L^2_x} + \beta\|\partial_x u_0\|^2_{L^2_x}. \tag{12}$$

Hence the solution cannot blow up in $H^1(\mathbb{R})$ in finite time and the proof of the proposition is complete. □

Remark 2.2. For more regular initial data, say for initial data u_0 in $H^2(\mathbb{R})$, we can prove similarly that there exists a unique global solution $u(t,x)$ in $C(0,+\infty;H^2(\mathbb{R}))$.

Remark 2.3. Energy equality (12) shows that the solution decays in a H^1 equivalent norm that reads $\sqrt{E}$ with $E = \|u(t)\|^2_{L^2} + \beta\|u_x(t)\|^2_{L^2}$. In fact E is a Lyapunov function which decays along the trajectories and that is constant only if $u(t,x) = C = 0$. Therefore all solutions converge to 0 when t goes to the infinity.

2.2. Case $\beta = 0$

The equation with $\beta = 0$ is difficult to handle directly by modern methods (S. Vento, personal communication). Therefore we will use a limiting argument by letting $\beta \to 0^+$ to construct a solution to

$$u_t + u_x + D^{\frac{1}{2}}u + D^{-\frac{1}{2}}u_x + uu_x = 0, \tag{13}$$

supplemented with initial data u_0 in $H^1(\mathbb{R})$. The drawback of this method is that the result requires some smallness assumption on the gradient of initial data u_0.

Proposition 2.4. *There exists a constant $c > 0$ such that for any u_0 in $H^1(\mathbb{R})$ with $\|\nabla u_0\|_{L^2(\mathbb{R})} \le c$, there exists a unique global solution u to the Eq. (13) (Eq. (4) with $\beta = 0$) that belongs to $L^\infty(0, +\infty; H^1(\mathbb{R}))$ and that satisfies the energy equality for any $t \ge 0$*

$$\|u(t)\|_{L^2}^2 + 2\int_0^t \|D^{\frac{1}{4}}u(s)\|_{L_x^2}^2 ds = \|u_0\|_{L_x^2}^2. \tag{14}$$

Proof. The proof is divided into three steps.

Step 1: existence proof. We begin with some a priori estimates for smooth solutions to (4). Considering u_0 in $H^2(\mathbb{R})$ and using Remark 2.2, there exists a solution $u(t, x) \in C(0, +\infty; H^2(\mathbb{R}))$. Multiplying (4) with $-2u_{xx}$ and integrating by parts, one obtains

$$\frac{d}{dt}\left(\|u_x\|_{L_x^2}^2 + \beta\|u_{xx}\|_{L_x^2}^2\right) + 2\|D^{\frac{5}{4}}u\|_{L_x^2}^2 = -\int_{\mathbb{R}} u_x^3 dx. \tag{15}$$

Now using the Gagliardo–Nirenberg inequality

$$\|\phi\|_{L_x^3}^3 \le c_1\|\phi\|_{L_x^2}\|D^{\frac{1}{4}}\phi\|_{L_x^2}^2, \tag{16}$$

with $\phi = u_x$, $\left|\int_{\mathbb{R}} u_x^3 dx\right|$ can be bounded from above by $c_1\|u_x\|_{L_x^2}\|D^{\frac{5}{4}}u\|_{L_x^2}^2$. Therefore

$$\frac{d}{dt}\left(\|u_x\|_{L_x^2}^2 + \beta\|u_{xx}\|_{L_x^2}^2\right) \le \left(c_1\|u_x\|_{L_x^2} - 2\right)\|D^{\frac{5}{4}}u\|_{L_x^2}^2. \tag{17}$$

Assume now that u_0 satisfies $c_1\|(u_0)_x\|_{L_x^2} < 2$. Then if $c_1\|u_x(t)\|_{L_x^2} \le 2$, $\|u_x\|_{L_x^2}^2 + \beta\|u_{xx}\|_{L_x^2}^2$ is decreasing with respect to t. Hence for β small enough depending on u_0 such that $\|(u_0)_x\|_{L_x^2}^2 + \beta\|(u_0)_{xx}\|_{L_x^2}^2 \le \frac{2}{c_1}$ the estimate $c_1\|u_x(t)\|_{L_x^2} \le 2$ is valid as long as the solution exists. Therefore we have a bound in $L^\infty(0, +\infty; H^1(\mathbb{R}))$ that does not depend on β. Going back to the equation we have

$$u_t = (1 - \beta\Delta)^{-1}\left(-\Lambda u - \frac{1}{2}\partial_x(u^2)\right).$$

Since $(1 - \beta\Delta)^{-1}$ is bounded as an operator in any Sobolev space H_x^s, it is easy to see that u_t remains in a bounded set of $L^\infty(0, +\infty; H^{-1}(\mathbb{R}))$ uniformly in β. Let u^β connote this solution. In order to pass the limit $\beta \to 0$, we first prove the following.

Lemma 2.5. *Fix $T > 0$. Consider a sequence u^β bounded in $L^\infty(0, T; H^1\mathbb{R})$ such that u_t^β remains bounded in $L^\infty(0, T; H^{-1}(\mathbb{R}))$. Then there exists a subsequence that converges strongly in $C(0, T; L_{\mathrm{loc},x}^2)$.*

Proof. Consider a sequence of smooth cut-off functions θ_n that satisfy $\theta_n = 1$ for $|x| \le n$ and whose support is included in $K_n = [-n-1, n+1]$. For any given n the sequence $\theta_n u^\beta$ is bounded in $X = \{v \in L^\infty(0, T; H_0^1(K_n)); v_t \in L^\infty(0, T; H^{-1}(K_n))\}$. The embedding $X \subset C(0, T; L^2(K_n))$ is compact (see [9]). Then by the Cantor diagonal process we can extract a subsequence that converges in $C(0, T; L_{\mathrm{loc},x}^2)$. $\square$

Applying this compactness argument allows us to pass to the limit in the nonlinear term. Actually, for any test function ϕ in the Schwartz class, we can pass to the limit in

$$\int_{\mathbb{R}} u_t^\beta(1 - \beta\Delta)\phi dx + \int_{\mathbb{R}} u^\beta(D^{\frac{1}{2}} - D^{-\frac{1}{2}}\partial_x - \partial_x)\phi dx = \int_{\mathbb{R}} (u^\beta)^2\phi_x dx. \tag{18}$$

Hence we have a weak solution to the equation that belongs to $L^\infty(0, +\infty; H^1(\mathbb{R}))$. The energy inequality (14) is obtained from (12) by a limiting argument.

Step 2: uniqueness proof. Consider $w = u - v$ which is the difference between two solutions of (13) that satisfy $c_1 \max_t \|u_x\| \leq 2$. Then w satisfies

$$w_t + \Lambda w + \partial_x \left(\frac{u+v}{2} w \right) = 0. \tag{19}$$

Multiply this equality by w and integrate by parts to obtain

$$\frac{d}{dt} \|w\|_{L_x^2}^2 + 2\|D^{\frac{1}{4}} w\|_{L_x^2}^2 = -\frac{1}{2} \int_{\mathbb{R}} (u_x + v_x) w^2 dx. \tag{20}$$

Using Cauchy–Schwarz and Sobolev embedding $H_x^{\frac{1}{4}} \subset L_x^4$ we have

$$\|w\|_{L_x^4}^2 \leq c_2 (\|w\|_{L_x^2}^2 + \|D^{\frac{1}{4}} w\|_{L_x^2}^2),$$

and then

$$\left| \frac{1}{2} \int_{\mathbb{R}} (u_x + v_x) w^2 dx \right| \leq c_2 \max(\|u_x\|_{L_t^\infty L_x^2}, \|v_x\|_{L_t^\infty L_x^2}) (\|w\|_{L_x^2}^2 + \|D^{\frac{1}{4}} w\|_{L_x^2}^2). \tag{21}$$

Therefore if u_0 (and v_0) satisfies $\max(c_1, c_2)\|u_0\|_{L_x^2} < 2$ we infer that

$$\frac{d}{dt} \|w\|_{L_x^2}^2 \leq \max(c_1, c_2) \|w\|_{L_x^2}^2, \tag{22}$$

and then by the Gronwall lemma

$$\|u(t) - v(t)\|_{L_x^2}^2 \leq \exp(\max(c_1, c_2)t) \|u_0 - v_0\|_{L_x^2}^2. \tag{23}$$

This implies uniqueness.

Step 3: relaxing the assumption on u_0 in the existence proof. Using the uniqueness result, we can relax the assumption u_0 in H_x^2 used in the existence process. For any u_0 in H_x^1, such that $\|\nabla u_0\|_{L_x^2}$ is small enough, we modify this initial condition to construct the approximating sequence. Since u belongs to $L_t^\infty H_x^1$ and u_t to $L_t^\infty H_x^{-1}$, u is continuous in t with values in $L^2(\mathbb{R})$ (see Lemma II 3.2 in [10]) and due to Strauss theorem (see Lemma II 3.3 in [10]) u is weakly continuous in t with values in $H^1(\mathbb{R})$. Going back to energy equality (14) that reads for $0 \leq t_0 < t$

$$\|u(t)\|_{L^2}^2 + 2 \int_{t_0}^{t} \|D^{\frac{1}{4}} u(s)\|_{L_x^2}^2 ds = \|u(t_0)\|_{L_x^2}^2, \tag{24}$$

we observe that the map $t \mapsto \|u(t)\|_{H_x^1}$ is continuous and therefore u is strongly continuous in t with values in $H^1(\mathbb{R})$. $\square$

2.3. Decay rate when viscous terms lead the dynamic ($\beta = 0, \gamma = 0$)

From the energy equality (24) in the section above, it transpires that the solution decays to 0 when time goes to $+\infty$ since $t \mapsto \|u(t)\|_{L_x^2}^2$ is a Lyapunov function that is constant only if $u = 0$. At this stage we are not able to compute theoretically the decay rate for the solutions, but we surmise that the linear part of the equation monitors the decay rate since the nonlinearity is asymptotically weak (see [11]).

We now address the decay rate issue for solutions to the linearized equation

$$u_t + u_x + D^{\frac{1}{2}} u + D^{-\frac{1}{2}} u_x = 0.$$

Using Fourier transform and Plancherel identity, we have

$$\|u(t)\|_{L^2(\mathbb{R})} = \left(\frac{1}{2\pi} \int_{\mathbb{R}} e^{-2t|\xi|^{\frac{1}{2}}} |\widehat{u}_0(\xi)|^2 d\xi \right)^{\frac{1}{2}} \leq c \|\widehat{u}_0\|_{L^\infty} t^{-1}. \tag{25}$$

Therefore, the L^2-norm of the linearized equation decays like t^{-1}. Analogously

$$\|u(t)\|_{L^\infty(\mathbb{R})} \leq \frac{1}{2\pi} \int_{\mathbb{R}} e^{-t|\xi|^{\frac{1}{2}}} |\widehat{u}_0(\xi)| d\xi \leq c \|\widehat{u}_0\|_{L^\infty} t^{-2}. \tag{26}$$

3. Boundary effects on the decay rates

To compute numerically the decay rate of solutions of a dispersive dissipative equation on the whole line, a finite space interval is often used with the assumption that values of the solution at the boundary are negligible. For wave equations, including dispersive conservative equations, it is well known that we have to perform the computations on a large enough interval. This is because the nonlocal term in the linear differential operator tends to spread out the solution on the whole line (and then boundary conditions matter), and the nonlinear term mixes frequencies in Fourier space.

Even with a large enough interval, the boundary conditions do matter in many circumstances. For example, it is known that KdV like equations on the periodic torus do not have the same dispersive properties as the same equation on the whole line. In the sequel we emphasize a difficulty related to the dissipation term, which provides polynomial decay towards equilibrium on the whole line and exponential decay towards the mean value in the periodic setting. This last difficulty occurs even for the linear equation and has a strong effect on how one collects data in the numerical simulation.

After fixing a large enough interval, say with size L, one assumes the solution at the boundary is negligible, the computation is then carried out for $t \to +\infty$ to obtain the decay rate for the solution. But when $t \to +\infty$, the solution at the boundary may not be negligible and the computed rate of decay is no longer an accurate approximation to the decay rate of the solution on the whole line. Therefore, there is a balance between the computational interval (large enough) and the time T (not infinitely large) where the data for obtaining decay rate of solutions to the whole line problem are collected (see Section 4.3 for more detail). When the data are indeed collected from $t \to +\infty$, the decay rate for the solution to the periodic boundary value problem could be obtained with a change of code since the equilibrium solution is the mean value, instead of 0.

We now perform a rigorous analysis for the following linear problem (with $\nu = 1$ and $\beta = \gamma = 0$ in (1)) that reads

$$u_t + u_x + D^{\frac{1}{2}} u + D^{-\frac{1}{2}} u_x = 0; \tag{27}$$

with initial condition

$$u(x, 0) = u_0(x), \quad x \in \mathbb{R}. \tag{28}$$

Proposition 3.1. *We consider a smooth initial data u_0 that is compactly supported, say in $[-1, 1]$. Let $u(t)$ be the solution of (27)–(28). Consider also the solution $U(t)$ to Eq. (27) on the periodic box ($L > 1$) $[-L, L]$, supplemented with initial condition u_0. Then there exists a constant C that depends on u_0 such that*

$$\left| \|u(t)\|^2_{L^2(\mathbb{R})} - \|U(t)\|^2_{L^2([-L,L])} \right| \leq \frac{C}{L}\left(1 + \frac{1}{t^2}\right). \tag{29}$$

Remark 3.2. Since the expected decay rate for $\|u(t)\|^2_{L^2(\mathbb{R})}$ is t^{-2} (say for $t \geq T$) from the linear analysis (25), then L has to be chosen large enough, such that $L \gg T^2$, for $\|U(t)\|^2_{L^2([-L,L])}$ and $\|u(t)\|^2_{L^2(\mathbb{R})}$ to have the same decay rate. It is worth to compare this error estimate with the case for the heat equation. For the heat equation, the error estimate (29) is the same and the expected decay rate for $\|u(t)\|^2_{L^2(\mathbb{R})}$ is $t^{-\frac{1}{2}}$. Therefore the corresponding requirement for L would be $L \gg T^{\frac{1}{2}}$. That means roughly that if a computational domain with $L = 10$ is enough to the heat equation, then a domain with $L = 10^4$ is needed for the Kakutani–Matsuuchi operator. For people that prefer to think of computing in fixed boxes, but with various viscosity parameters, we remind that there exist a relationship between $\nu\Delta$ on $[0, 1]$ and Δ on $[0, L]$ that reads $\nu L^2 = 1$ with heat equation. For Kakutani–Matsuuchi operator the scaling is $\nu L^{\frac{1}{2}} = 1$.

Remark 3.3. The same results apply also if we do not assume that u_0 is compactly supported but in the Schwartz class such that the following estimate is valid

$$|u_0(x)| \leq c e^{-2|x|}. \tag{30}$$

Actually, this provides us with a new error term that is as small as $\exp(-L)$ and that does not alter the result. For the sake of conciseness, we omit the computations that are standard. The assumption (30) amounts to assume that the Fourier transform of u_0 has compact support, due to the Paley–Wiener-Schwartz theorem. This particular case is consistent with the choice of initial data chosen for the numerical simulation performed in the next section.

Proof of Proposition 3.1. Since we are interested in the L^2 decay estimate, the skew-symmetric part of the linear operator $u_x + D^{-\frac{1}{2}} u_x$, does not play a role (see formula (25) for instance). We therefore analyze the solutions of the dissipative equation

$$u_t + D^{\frac{1}{2}} u = 0; \qquad u(x, 0) = u_0(x), \quad x \in \mathbb{R}. \tag{31}$$

Here we have assumed $\nu = 1$ without loss of generality since L and ν are related by a scaling relation.

Let us introduce the periodic function, that is a carbon copy of u_0,

$$U_0(x) = \sum_{j \in \mathbb{Z}} u_0(x + 2jL). \tag{32}$$

Due to the Poisson summation formula, its Fourier coefficient

$$U_0^k = \frac{1}{2L}\int_{-L}^{L} U_0(x)\exp\left(-\frac{ik\pi x}{L}\right)dx \tag{33}$$

satisfies $U_0^k = \frac{1}{2L}\widehat{u}_0\left(\frac{k\pi}{L}\right)$ where $\widehat{u}_0$ is the Fourier transform of u_0.

Let us recall that solving the PDE with periodic boundary conditions and initial data U_0 amounts to computing

$$U(t)(x) = U(t,x) = \sum_{k\in\mathbb{Z}} e^{-t\sqrt{\frac{k\pi}{L}}} U_0^k e^{\frac{i\pi kx}{L}}. \tag{34}$$

On the one hand, using the Plancherel formula, we have that

$$\|u(t)\|^2_{L^2(\mathbb{R})} = \frac{1}{2\pi}\int_{\mathbb{R}} e^{-2t|\xi|^{\frac{1}{2}}}|\widehat{u}_0(\xi)|^2 d\xi. \tag{35}$$

On the other hand, from (31), (34) and Parseval identity,

$$\|U(t)\|^2_{L^2(-L,L)} = \sum_{k\in\mathbb{Z}} \frac{1}{2L} e^{-2t|\frac{k\pi}{L}|^{\frac{1}{2}}} |\widehat{u}_0\left(\frac{k\pi}{L}\right)|^2. \tag{36}$$

Therefore, if $\varepsilon = |\ \|u(t)\|^2_{L^2(\mathbb{R})} - \|U(t)\|^2_{L^2(-L,L)}\ |$, then

$$\varepsilon = \left|\frac{1}{2\pi}\int_{\mathbb{R}} e^{-2t|\xi|^{\frac{1}{2}}}|\widehat{u}_0(\xi)|^2 d\xi - \sum_{k\in\mathbb{Z}}\frac{1}{2L}e^{-2t\left|\frac{k\pi}{L}\right|^{\frac{1}{2}}}\left|\widehat{u}_0\left(\frac{k\pi}{L}\right)\right|^2\right|, \tag{37}$$

which is the approximation error of the integral by the rectangle formula.

Let $\phi(\xi) = e^{-2t|\xi|^{\frac{1}{2}}}|\widehat{u}_0(\xi)|^2$, we will bound $\varepsilon = \sum_{k\in\mathbb{Z}}\varepsilon_k$ using

$$\varepsilon_k = \left|\int_{\frac{k\pi}{L}}^{\frac{(k+1)\pi}{L}}\left(\phi(\xi) - \phi\left(\frac{k\pi}{L}\right)\right)d\xi\right| \le \frac{c}{L}\min(\|\phi\|_{L^\infty(I_k)}, L^{-1}\|\phi'\|_{L^\infty(I_k)}).$$

For $k = 0$,

$$\varepsilon_0 \le \frac{c}{N}; \tag{38}$$

and for $k \neq 0$,

$$\varepsilon_k \le cL^{-2}\exp\left(-t\sqrt{\frac{|k|\pi}{L}}\right)\left(1 + t\sqrt{\frac{L}{|k|\pi}}\right). \tag{39}$$

We then have

$$\sum_{k\neq 0}\varepsilon_k \le 2cL^{-2}\sum_{k=1}^{+\infty}\exp\left(-t\sqrt{\frac{k\pi}{L}}\right)\left(1 + t\sqrt{\frac{L}{k\pi}}\right). \tag{40}$$

Therefore

$$\sum_{k\neq 0}\varepsilon_k \le 2cL^{-2}\int_0^{+\infty}\exp\left(-t\sqrt{\frac{x\pi}{L}}\right)\left(1 + t\sqrt{\frac{L}{x\pi}}\right)dx \le 2\tilde{c}L^{-2}\left(\frac{L}{t^2} + L\right). \tag{41}$$

Gathering (38) and (41) completes the proof of the proposition. □

4. Numerical study

4.1. The numerical scheme

We describe in this subsection the numerical scheme for simulating solutions of (1).

For the time discretization, a semi-implicit Crank–Nicholson-leapfrog method (with the first step computed by a semi-implicit backward Euler method) is used in order to have a conservative scheme if $\nu = \beta = \gamma = 0$ (for more details, see [12]). More precisely, let δt be the time step and $t^n = n\delta t$ for $n \in \mathbb{N}$, the scheme can be written, for $n \geq 1$

$$(1-\beta\Delta)\frac{u^{n+1}-u^{n-1}}{2\delta t} + \nu G^n(u) + \frac{1}{2}(u_x^{n+1}+u_x^{n-1}) + \gamma u^n u_x^n = 0, \tag{42}$$

where u^n represents the numerical approximation of $u(t^n, \cdot)$ and u^0 is the initial data u_0. The dissipative and dispersive term $G^n(u)$ at time t^n with $G^n(u) = (D^{\frac{1}{2}}u + \mathcal{F}^{-1}(i|\xi|^{\frac{1}{2}}\operatorname{sgn}(\xi)\widehat{u}(\xi)))^n$ is approximated by

$$\widetilde{G}^n(u) = \frac{1}{2}D^{\frac{1}{2}}(u^{n-1}+u^{n+1}) + \mathcal{F}^{-1}\left(\frac{1}{2}i|\xi|^{\frac{1}{2}}\operatorname{sgn}(\xi)(\widehat{u}^{n-1}(\xi)+\widehat{u}^{n+1}(\xi))\right). \tag{43}$$

For the space discretization, a Fourier discretization is implemented, so Fast Fourier Transforms can be used. Therefore, the periodic boundary condition with large L, which is the length of the computational domain, is used.

The fully discretized problem can be written, with $\widehat{u}(\xi)$ denoting the Fourier transform of u at the frequency ξ, for $n \geq 1$

$$(1+\beta\xi^2)(\widehat{u}^{n+1}-\widehat{u}^{n-1}) + \nu\delta t|\xi|^{\frac{1}{2}}(1+i\operatorname{sgn}(\xi))(\widehat{u}^{n-1}+\widehat{u}^{n+1}) + i\delta t\xi\left(\widehat{u}^{n+1}+\widehat{u}^{n-1}+2\gamma\, FFT\left(\frac{(u^n)^2}{2}\right)\right) = 0 \tag{44}$$

at time $t^n = n\delta t$, and for $\xi = \frac{2\Pi}{L}j$, $-\frac{N}{2} \leq j \leq \frac{N}{2}$ where N is the number of modes used in the simulation.

4.2. Validation of the scheme

In order to validate the numerical method used in the sequel, we will follow the ideas of Chen [12]. This technique consists of neglecting the viscous term in Eq. (4), and computing numerically the solution of this equation with a known exact solitary-wave solution. With $\nu_1 = \nu_2 = 0$, $\beta = \gamma = 1$, Eq. (4) reads

$$u_t + u_x - u_{txx} + uu_x = 0.$$

Let $u(x,t) = \phi(x-pt)$, ϕ satisfies

$$(p-1)\phi' - p\phi''' - \phi\phi' = 0.$$

Using Lemma 1 in [13], namely $\alpha\eta' - \beta\eta''' - \eta\eta' = 0$ admits a solution $\eta = 3\alpha\,\operatorname{sech}^2\left(\frac{1}{2}\sqrt{\frac{\alpha}{\beta}}x\right)$, one finds explicit solutions

$$u(x,t) = \phi(x-pt) = 3(p-1)\ \operatorname{sech}^2\left(\frac{1}{2}\sqrt{\frac{p-1}{p}}(x-pt)\right). \tag{45}$$

The one with $p = 2$ is used for our testing.

For an interval of length $L = 400$ with $N = 800$ mode, a time step $\delta t = 0.01$, the computed solution has $\|u(T,\cdot)\|_{L^\infty}$ equal to 3.00005 at $T = 50$ while the explicit solution has $\|u_{ex}(T,\cdot)\|_{L^\infty}$ equal to 3. The maximum difference between the computed solution $u(T,\cdot)$ and $u_{ex}(T,\cdot)$ at $T = 50$, $\|u_{ex}(T,\cdot) - u(T,\cdot)\|_{L^\infty}$ is equal to 1.17×10^{-4}. By halving the size of δt to 0.005, $\|u_{ex}(T,\cdot) - u(T,\cdot)\|_{L^\infty}$ decreased to 2.91×10^{-5}. Therefore, the numerical scheme is validated for non-dissipative equation and it is second order in time as expected. It has a spectral accuracy in space.

4.3. The influence of the computational domain and other computational parameters

Since the solution is expected to decay in the form of $O(t^a)$, namely $\|u(t,\cdot)\|_{L_x^2} \approx Ct^{\alpha_2}$ or $\|u(t,\cdot)\|_{L_x^\infty} \approx Ct^{\alpha_\infty}$ for t large, the ratios

$$R_2 = \frac{\log\frac{\|u(t,\cdot)\|_{L_x^2}}{\|u(t-\delta_1,\cdot)\|_{L_x^2}}}{\log\frac{t}{t-\delta_1}}, \quad \text{and} \quad R_\infty = \frac{\log\frac{\|u(t,\cdot)\|_{L_x^\infty}}{\|u(t-\delta_2,\cdot)\|_{L_x^\infty}}}{\log\frac{t}{t-\delta_2}}$$

are expected to approach respectively to the decay rates α_2 and α_∞ as $t \to \infty$.

To predict the decay rate α_2, the ratio R_2 was computed first for $t \in [0, 50]$ with $L = 400$ ($\delta_1 = 0.1$, $\nu = 0.1$, β and γ equal to 1, $\delta t = 10^{-2}$, $h = 2 \times 10^{-2}$). It was observed that the minimum value of R_2 was -0.79 and R_2 was not approaching constant. By carrying the computation to $T = 300$, we found R_2 approaching 0 instead of -1, the expected result (see Fig. 1). The value of R_2 made a turn at t close to 45, still with the minimum -0.79. This observation inspired the analysis performed in Section 3 which made us realize that L has to be taken large enough and T should be taken in a range which depends on L. The influence of L is then investigated in Fig. 1 for $L = 400, 1000, 5000, 10\,000, 20\,000, 30\,000$. It is clear that for $T = 300$, the L has to be larger than 20 000 to obtain the correct rate of decay. If L is smaller than 1000, the boundary effect starts to influence the result and the correct decay rate cannot be obtained. With $L > 20\,000$, T from [100, 300] gives the best approximation.

A similar plot is made for the L^∞-norm but with $\delta_2 = 10$ which is much larger than δ_1, see Fig. 2. If δ_2 was the same as δ_1, the curves would have oscillations because the location of the mesh points. If the peak belongs to the mesh points, then

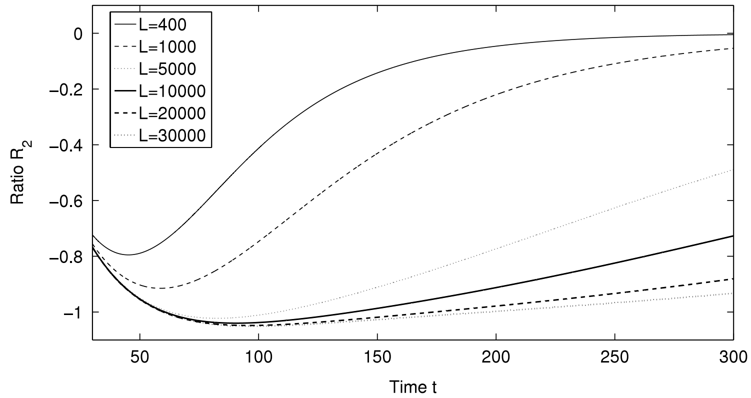

Fig. 1. Ratio R_2 versus the time t for numerical solutions computed on domains $[0, L]$ for L ranging from 400 to 30 000 ($\nu = 0.1$, $\beta = \gamma = 1$).

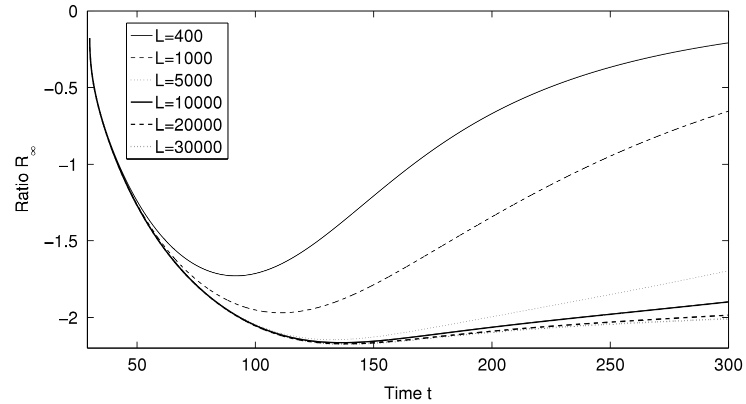

Fig. 2. Ratio R_∞ versus the time t for numerical solutions computed on domains $[0, L]$ for L ranging from 400 to 30 000 ($\nu = 0.1$, $\beta = \gamma = 1$).

Table 1
Values of $\frac{u(T=300,L)}{\|u(T=300,\cdot)\|_{L^\infty}}$ for various values of L which indicate the influence of the boundary condition on the decay rate of the solution.

L	$\frac{u(T=300,L)}{\|u(T=300,\cdot)\|_{L^\infty}}$
400	9.43×10^{-1}
1 000	8.39×10^{-1}
5 000	1.50×10^{-1}
10 000	5.73×10^{-2}
20 000	2.09×10^{-2}
30 000	1.15×10^{-2}

the numerical L^∞-norm is bigger than when the peak is not on the mesh points, even for the same solution. This fluctuates then generates the oscillation on the curve when δ_2 is small.

Since the main reason for the large L is the spread of the solution to the boundary, the solution on $\mathbb{R}$ is very different from the solution on the bounded domain $[0, L]$ for a small value of L, it is useful to know quantitatively the size of the solution at the boundary. Table 1 presents the values of $\frac{u(T,L)}{\|u(T,\cdot)\|_{L^\infty}}$ for various values of L, where $u(T, \cdot)$ is the solution computed on the domain $[0, L]$.

The results on Table 1 shows that $\frac{u(T,L)}{\|u(T,\cdot)\|_{L^\infty}}$ is decreasing with L, and a ratio less than 10^{-2} seems to be sufficient to obtain the good decay.

In summary, careful consideration needs to be taken for choosing L and T to find the decay rate of the solution for a Cauchy problem with non-local operator. In many cases, numerous experiments have to be performed.

4.4. Decay rate for various values of the parameters

Since we can only prove analytically the decay rates for $\beta = 0$ and $\gamma = 0$, numerical simulations are performed to compute the decay rates, both with the L^2 and L^∞ norm. In this computation, the domain of computation in space is $\Omega = [0, 20\,000]$, the space step of discretization is $h = 2 \times 10^{-2}$, the time step of discretization is $\delta t = 10^{-2}$, and the initial datum is the BBM soliton (45) with $p = 2$.

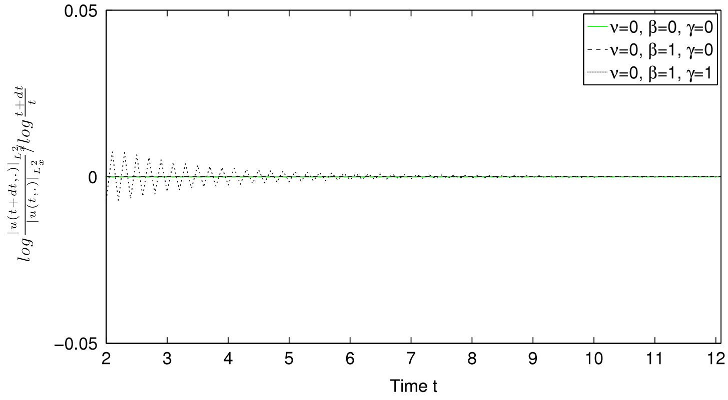

Fig. 3. Ratio R_2 versus the time t for various values of parameters β and γ $(\nu = 0)$. The three curves overlap each other, so there is no dissipation if $\nu = 0$.

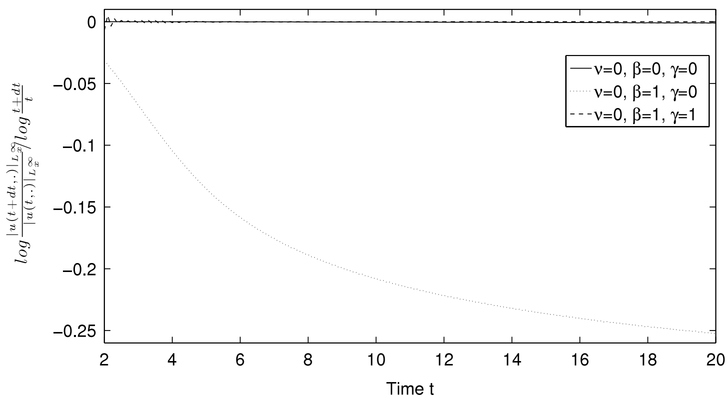

Fig. 4. Ratio R_∞ versus the time t for various values of parameters β and γ $(\nu = 0)$. The first and the third curves overlap each other because the initial datum provides a soliton in the third case.

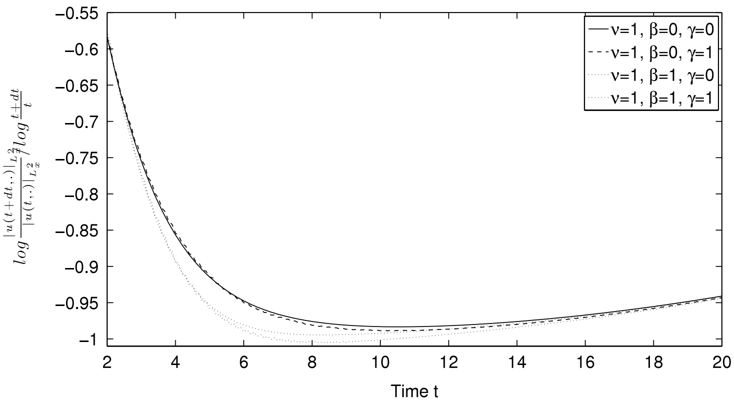

Fig. 5. Ratio R_2 versus the time t for various values of parameters β and γ $(\nu = 1)$. It shows that the non-local term provides dissipation.

The ratios R_2 and R_∞ versus the time t are plotted in Figs. 3 and 4 for $\nu = 0$. It shows that if $\nu = \beta = \gamma = 0$ (wave equation), the scheme is able to observe that this equation is conservative, both in the L^2 and L^∞ norms. For all the cases with $\nu = 0$, the decay rate for L^2-norm is 0. There is decay in L^∞ when the dispersion term is not balanced by the nonlinear term. Figs. 5 and 6 are for $\nu = 1$, which predict that when the viscosity occurs, the decay rate is equal to -1 in the L^2 norm, and to -2 in the L^∞ norm. The values of the decay rate are presented in Table 2 where the data are the minimum values of $R_2(t)$ and $R_\infty(t)$. It shows that as predicted by the linear analysis, the non-local term does provide dissipation and dispersion.

4.5. Influence of the magnitude of the viscosity

In this subsection, numerical experiments are performed to study the influence of the viscosity on the decay rate. In these simulations, the computational parameters are: $L = 16\,000$, $h = 2 \times 10^{-2}$, $\delta t = 10^{-2}$, $T = 20$, $\beta = \gamma = 1$. In these experiments, the initial datum is the function (45) with $p = 2$, and shift around the point $x_0 = 8000$.

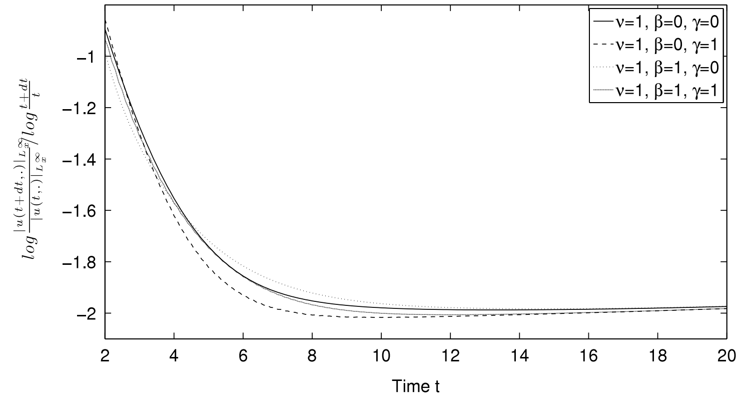

Fig. 6. Ratio R_∞ versus the time t for various values of parameters β and γ ($\nu = 1$), so the viscosity also provides dispersion.

Table 2
Decay rate of the solution $u(t, \cdot)$ versus the time.

Viscosity ν	Dispersive term β	Non linear term γ	L^2decay rate	L^∞decay rate
0	0	0	10^{-14}	10^{-3}
0	1	1	10^{-14}	0.01
1	0	0	−0.98	−1.94
1	0	1	−0.92	−2.00
1	1	0	−1.00	−1.91
1	1	1	−0.97	−1.95

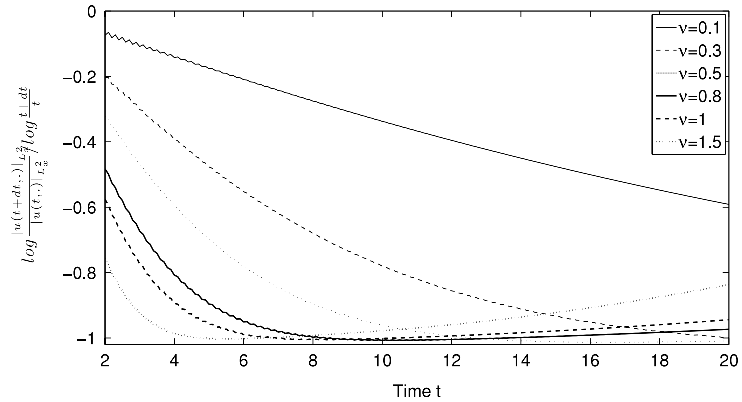

Fig. 7. Ratio R_2 versus the time t for ν ranging from 0.1 to 1.5.

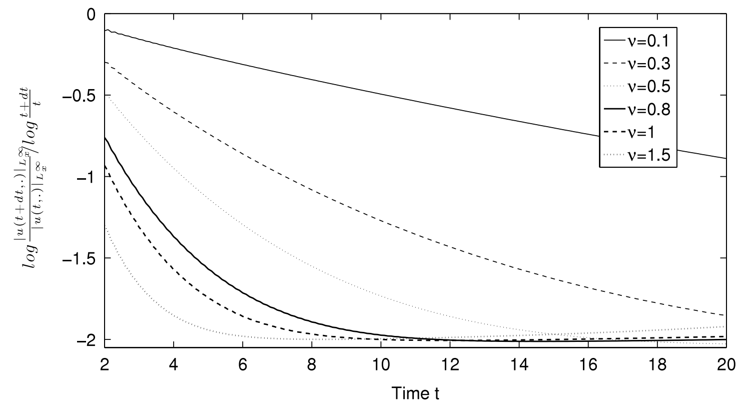

Fig. 8. Ratio R_∞ versus the time t for ν ranging from 0.1 to 1.5.

Figs. 7 and 8 show that if the viscosity is small (ν equal to 0.1), a large time is required to obtain the correct decay rate. When the viscosity increases, the expected decay rates −1 for the L^2 norm and −2 for the L^∞ norm can be obtained with relatively small t. When t increases more, the curve starts to going up, due to the boundary influence described in the previous section.

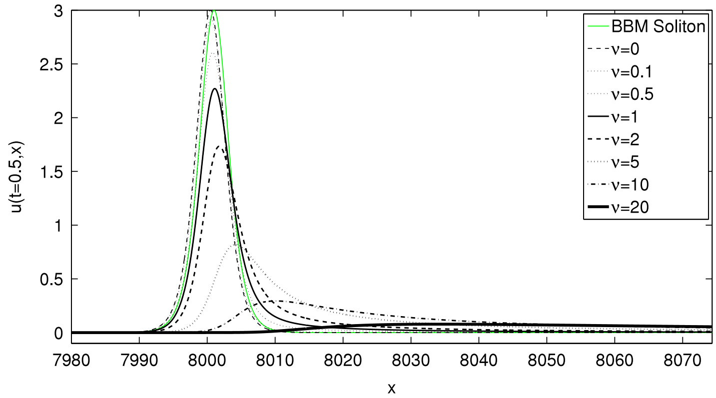

Fig. 9. Solutions for the viscosity ν ranging from 0 to 20.

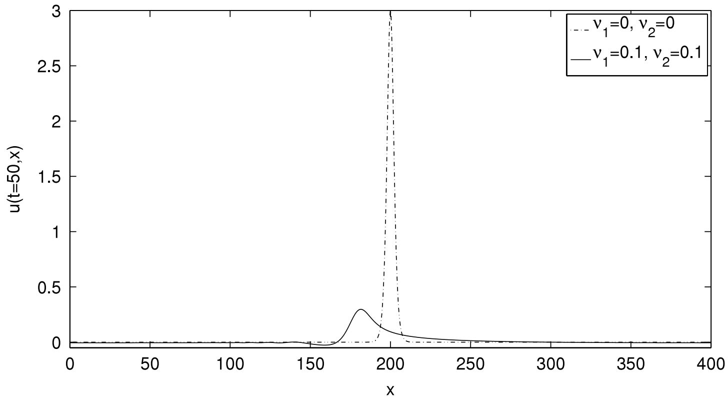

Fig. 10. Cumulative influence of ν_1 and ν_2 on a computed solution with $\beta = \gamma = 1$, at time $t = 50$ for various viscosities: $\nu_1 = \nu_2 = 0$ (dashed line) and $\nu_1 = \nu_2 = 0.1$ (solid line).

The solutions at $t = 0.5$ for equations with various ν between 0 and 20 are plotted in Fig. 9. As expected, there is more damping for larger ν. In addition, one observes that the velocity of the wave also increases with the viscosity.

4.6. Relative influence of the two terms in the viscosity

In this subsection, the viscosity in (1) is split into two parts:

$$G(u) = \nu_1 D^{\frac{1}{2}} u + \nu_2 \mathcal{F}^{-1}\left(i|\xi|^{\frac{1}{2}} \operatorname{sgn}(\xi)\widehat{u}(\xi)\right) \tag{46}$$

in order to study the relative influence of each part.

By taking $\nu_1 = \nu_2 = 0.1$, we computed the solution at $T = 50$ again with the same initial data ($x_0 = 100$), which is plotted with a solid line in Fig. 10. For comparison, the solutions without the non-local dispersive and dissipative terms ($\nu_1 = \nu_2 = 0$) are also plotted with the dashed line. The dissipative effect of the terms is quite clear. The peak of the solution drops from 3 to 0.3545, and the L^2-norm of the solution drops from 5.8259 to 1.5266.

Now looking at the effect of each individual term, we first take $\nu_1 = 0$ and $\nu_2 = 0.1$ and the solution is plotted in Fig. 11. The term $D^{-\frac{1}{2}} u_x$ actually speeds up the propagation. Here, the L^2-norm of the solution remains almost a constant.

The case with $\nu_1 = 0.1$ and $\nu_2 = 0$ is also investigated. The solution is plotted in Fig. 12 which shows the $D^{\frac{1}{2}} u$ slows the propagation down. With equal constants, this shows that the dissipation $D^{\frac{1}{2}} u$ has a stronger effect on the solution than the dispersive $D^{-\frac{1}{2}} u$ term. Here, the L^2-norm of the solution drops from 5.8259 to 1.444.

Figs. 13 and 14 shows that the equation is conservative in both two norms. The L^2-norm is conserved if $\nu_1 = 0$ and has a decay rate -1 when $\nu_1 = 1$. For L^∞-norm, the solution decays when either ν_1 and/or ν_2 is nonzero.

4.7. Conclusion

In this section, we have discussed the influence of the size of the domain. A large enough domain is required to provide the accurate decay estimates for solutions on the whole line. In addition, the numerical simulations are carried out and the results show that the nonlocal viscose term provides dissipation and the term "$D^{-\frac{1}{2}} u_x$" in the viscosity terms also provides

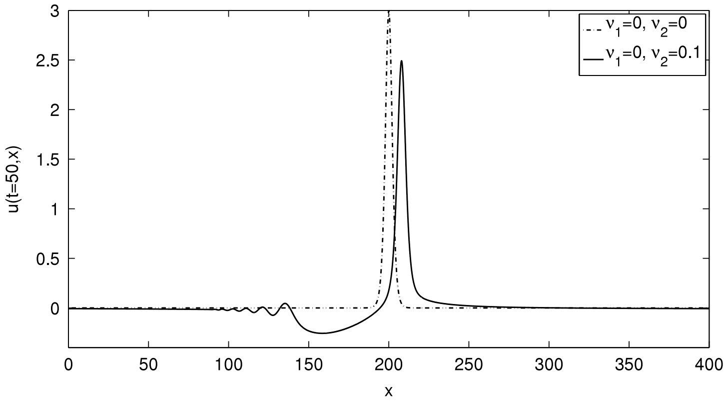

Fig. 11. Influence of ν_2 on computed solution with $\beta = \gamma = 1$, $\nu_1 = 0$ at time $t = 50$ for various viscosities: $\nu_2 = 0$ (dashed line) and $\nu_2 = 0.1$ (solid line).

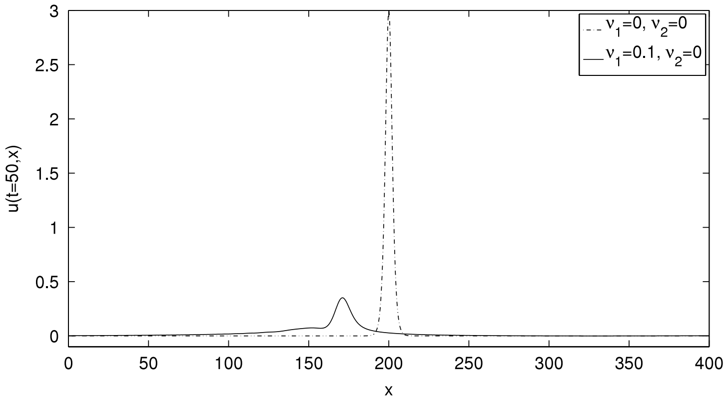

Fig. 12. Influence of ν_1 on computed solution with $\beta = \gamma = 1$, $\nu_2 = 0$ at time $t = 50$ for various viscosities: $\nu_1 = 0$ (dashed line) and $\nu_1 = 0.1$ (solid line).

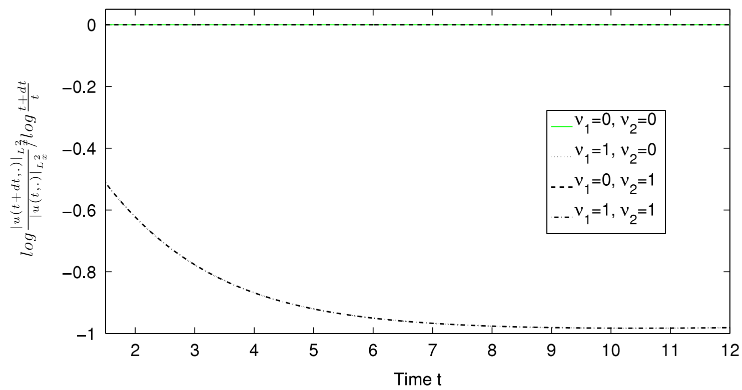

Fig. 13. Ratio R_2 versus the time t for the viscosities' coefficients ν_1 and ν_2 equal to 0 and 1. The first and third (resp. the second and the fourth) curves overlap each other, this figure shows that the parameter ν_1 is more significant on the L^2 decay of the solution.

dispersion. This numerical study also predicts the decay rates of the solutions for the whole system which include the nonlinear term $|u|u_x$ and the term $-u_{txx}$, which are $O\left(\frac{1}{t}\right)$ in the L^2 norm and $O\left(\frac{1}{t^2}\right)$ in the L^∞ norm, a result which has not been proved theoretically until now.

Acknowledgments

The present work was initiated when the two last authors were visiting the Math Department at Purdue University, with the support of the CNRS for the research exchange program *waterwaves*. The last author would like to thank S. Vento for discussions about the Kakutani–Matsuuchi equation. The authors would like to thank the anonymous referees for remarks that improved the present article. The first author was partially supported by a grant from the Simons Foundation (#198275 to Min Chen).

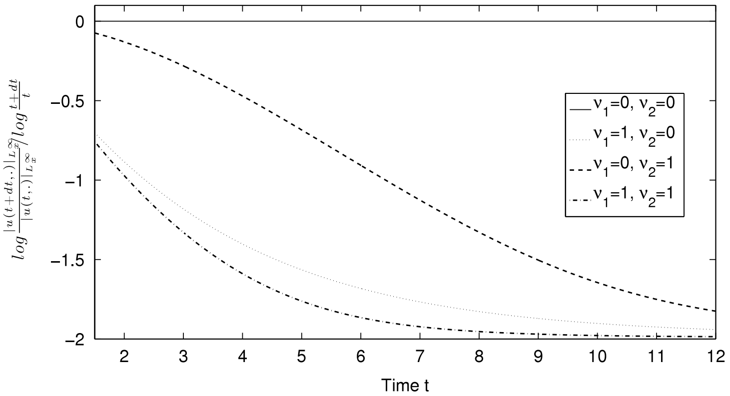

Fig. 14. Ratio R_∞ versus the time t for the viscosities' coefficients ν_1 and ν_1 equal to 0 and 1. The two parameters ν_1 and ν_2 act on the L^∞ decay of the solution.

References

[1] P. Liu, A. Orfilla, Viscous effects on transient long wave propagation, J. Fluid Mech. 520 (2004) 83–92.
[2] D. Dutykh, F. Dias, Viscous potential free surface flows in a fluid layer of finite depth, C.R.A.S Série I 347 (2007) 113–118.
[3] C.J. Amick, J.L. Bona, M.E. Schonbek, Decay of solutions of some nonlinear wave equations, J. Differential Equations 81 (1989) 1–49.
[4] J.L. Bona, K. Promislow, C.E. Wayne, Higher-order asymptotics of decaying solutions of some nonlinear, dispersive, dissipative wave equations, Nonlinearity 8 (6) (1995) 1179–1206.
[5] M. Chen, S. Dumont, L. Dupaigne, O. Goubet, Decay of solutions to a water wave model with a nonlocal viscous dispersive term, Discrete Contin. Dyn. Syst. 27 (4) (2010) 1473–1492.
[6] T. Kakutani, M. Matsuuchi, Effect of viscosity of long gravity waves, J. Phys. Soc. Japan 39 (1975) 237–246.
[7] J.L. Bona, F. Demengel, K. Promislow, Fourier splitting and dissipation of nonlinear dispersive waves, Proc. Roy. Soc. Edinburgh Sect. A 129 (3) (1999) 477–502.
[8] E. Ott, R.N. Sudan, Damping of solitary waves, Phys. Fluids 13 (1970) 1432–1434.
[9] L. Tartar, Topics in nonlinear analysis, Publ. Math. Orsay 13 (1978).
[10] R. Temam, Infinite-Dimensional Dynamical Systems in Mechanics and Physics, in: Applied Mathematical Sciences, vol. 68, Springer-Verlag, New York, Berlin, Heidelberg, 1988.
[11] N. Hayashi, E.I. Kaikina, P.I. Naumkin, I.A. Shishmarev, Asymptotics for Dissipative Nonlinear Equations, in: Lecture Notes in Mathematics, vol. 1884, Springer-Verlag, Berlin, 2006.
[12] M. Chen, Numerical investigation of a two-dimensional Boussinesq system, Discrete Contin. Dyn. Syst. 28 (4) (2009) 1169–1190.
[13] M. Chen, Exact traveling-wave solutions to bi-directional wave equations, Internat. J. Theoret. Phys. 37 (5) (1998) 1547–1567.

Further reading

[1] J.L. Bona, M. Chen, J.-C. Saut, Boussinesq equations and other systems for small-amplitude long waves in nonlinear dispersive media. Part II: the nonlinear theory, Nonlinearity 17 (3) (2004) 925–952.
[2] M. Chen, O. Goubet, Long-time asymptotic behavior of dissipative Boussinesq system, Discrete Contin. Dyn. Syst. 17 (3) (2007) 509–528.
[3] J.C. Eylbeck, G.R. McGuire, Numerical study of the regularized long-wave equation 1: numerical methods, J. Comput. Phys. 19 (1975) 43–57.